IEEE/CSC & ESAS European Superconductivity News Forum (ESNF), No. 15, January 2011
(ASC 2010 preprint 3MP2E-08 submitted to *IEEE Transactions on Applied Superconductivity* and pre-published by ESNF conforming to IEEE Policy on Electronic Dissemination, Section 8.1.9)

Fundamental evaluations of transverse load effects of Nb_3Sn strands using finite element analysis

T. Wang, L. Chiesa, and M. Takayasu

***Abstract*—The performances of large superconducting Cable-In-Conduit Conductors (CICC) are affected by various mechanical effects caused by thermal contractions during cooldown and the inherent interaction of current and field during operations. Recent large CICC cables and magnets such as ITER conductors have shown significant unexpected degradations. In this paper the transverse load effect caused by the Lorentz load is studied for a single strand and a 3-strand cable, basic elements of a CICC. 2D finite element models of Nb_3Sn single strand and 3-strand cable are developed to study the deformation and contact pressure of individual strand under external transverse loads. The strain and stress distributions of each strand inside a triplet are investigated considering the different positions of a strand in a triplet to simulate a twisted cable. The numerical results, combined with the single-strand experimental results and theory of contact mechanics, are applied to estimate the performance of a twisted 3-strand cable. The behavior of the 3-strand configuration obtained using finite element analysis (FEA) is discussed and compared to experimental results and existing models of the effect of contact pressures on the performance of superconducting cables.**

***Index Terms*—FEA, Nb_3Sn strands, transverse load, CICC**

I. INTRODUCTION

THE International Thermonuclear Experimental Reactor uses superconducting magnets, whose coils are made of superconducting Nb_3Sn Cable-in-Conduit Conductors (CICC). During operation, the Nb_3Sn strands are subjected to several types of loads: axial, bending and transverse load. The transverse load, caused by the natural Lorentz load, is believed to be one of the causes of the unexpected performance degradation of the Nb_3Sn CICC. Due to this reason, a transverse load hairpin experiment of the sub-size Nb_3Sn cable was carried out to study the effects of the transverse load on the performance of Nb_3Sn [1]. In this paper Finite Element Analysis (FEA) of single strand and triplet, the basic elements of CICC configuration, is carried out based on the simulation of this transverse load experiment. The simulation results are compared with the experimental results to investigate the strain in the strand(s) under transverse load and the relation between the performance of the strand(s) and the strain state in the strand(s).

Manuscript received 3 August 2010. This work was supported in part by the U.S. Department of Energy under Grant DE-SC00004062.

T. Wang and L. Chiesa are with the Department of Mechanical Engineering, Tufts University, Medford, MA 02155 USA (phone: 617-627-4575; e-mail: Tiening.Wang@tufts.edu, Luisa.Chiesa@tufts.edu)

M. Takayasu is with the Plasma Science and Fusion Center, Massachusetts Institute of Technology, Cambridge, MA 02139 USA (e-mail: takayasu@psfc.mit.edu)

II. FE METHODOLOGY

The FEA of the strand(s) under transverse load was carried out using ANSYS®. Because the axial length of the strand(s) is much longer than the diameter in the experiment, the analysis is considered as a 2D plane strain problem (Fig. 2). The strand(s) was modeled with PLANE183 elements. The pressing plates were also built to apply transverse compression onto the strand(s). CONTA172 and TARGE169 elements were used to describe contact behaviors.

The sample wire and the single strand finite element (FE) model are shown in Fig.1 and Fig. 2, respectively. Note that the diameter of the superconducting Nb_3Sn filaments is around 6 μm and the amount of these filaments is over 2500, which makes the modeling of individual filament very difficult and time consuming, therefore in FE models, these filaments and the bronze close to them are modeled as solid filament areas.

Because of the twist of the strands in the triplet around the longitudinal axis, the cross sections of the triplet are different

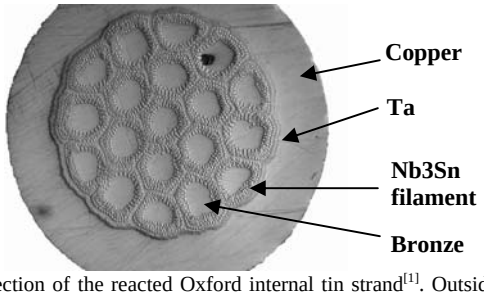

Fig. 1 The cross section of the reacted Oxford internal tin strand[1]. Outside diameter is 0.817 mm. The strand has 19 sub-elements.

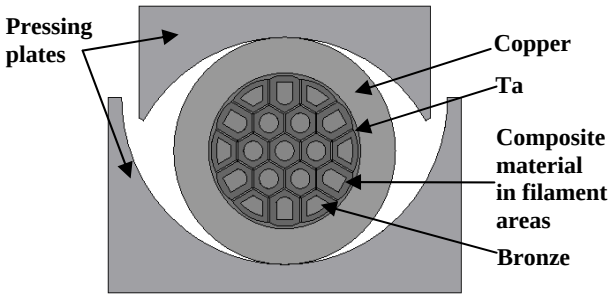

Fig. 2. FE model of the single strand and pressing plates. The composite material is composed of bronze and Nb_3Sn.

at different axial positions. Two cases of the cross section of the cable were modeled in the simulation: case A and case B,

shown in Fig. 3. The radius of the pressing plates is 0.88 mm. All strands are constrained by the contact pairs between the pressing plates and the strands, while the other contact pairs cover all possible contact regions between any two of the strands. The coefficient of friction is 0.2 for plate-strand (steel-copper) contacts and 1 for strand-strand (copper-copper) contacts [2].

To simulate the loading conditions, the inside edge of the upper plate is dispalced downward and fixed horizontally. The edge of the lower plate is fixed. In this way, the plates can be considered as rigid bodies. The displacement of the upper plate is up to 0.1 mm in the single strand case, 0.3 mm in case A and case B of the triplet.

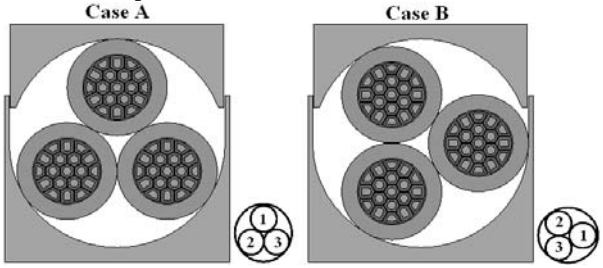

Fig. 3. FE model of case A and B of triplet with the numbering of the strands.

III. Material properties

In the simulation, a strand undergoes severe transverse compression and has plastic deformation. Therefore elastic-plastic stress-strain curves are used in the material modeling. The curves are described with two options in the simulation: Bi-linear Isotropic Hardening Option (BISO) and Multi-linear Isotropic Hardening Option (MISO) in ANSYS®.

The reacted Nb_3Sn strand is considered to have four materials: annealed copper, bronze, Nb_3Sn and Ta. The stress-strain curves of all materials except Nb_3Sn were calculated using Mitchell's equations at a temperature of 4 K [3]. All materials have elasto-plastic properties except Nb_3Sn. Copper and bronze are described with MISO while Ta is described with BISO. Nb_3Sn is assumed to be elastic under compression. M. Poirier measured the Young's modulus of Nb_3Sn ranging from 4 K to 300 K and found the value at 4 K is 49 GPa [4]. This value is used in the following calculation of the composite material.

As the filament areas have two materials: bronze and Nb_3Sn, composite material of bronze and Nb_3Sn is assigned to these areas. The rule of mixtures (ROM) can estimate the elastic modulus of the composite material but the stress-strain curve of bronze has plastic region. This means once bronze yields; the composite material has a non-linear behavior, which is not suitable for the use of the ROM. However, D.S. Easton and A. Nijhuis used the ROM to calculate the plastic modulus of the Nb_3Sn composite strand in longitudinal direction successfully, as in [5] and [6]. Therefore, this analysis uses the ROM to estimate the modulus of the composite material (bronze and Nb_3Sn) and the only difference from their applications is that the expression of the ROM in transverse direction is used since the strand(s) undergoes transverse load. All material stress-strain curves used in the simulations are plotted in Fig. 4.

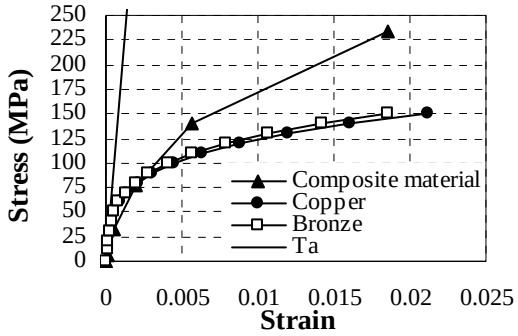

Fig. 4. The material properties used in the analysis.

IV. Results and Discussion

A. Single strand results

The experimental measurements of the displacement of the upper plate as a function of the applied force per unit axial length can be compared to the simulation. In the experiment, the radius of the plates may be larger than 0.4085 mm (the design value) due to the machining tolerances, therefore the simulations were carried out with the radius of the pressing plates R = 0.5, 0.6 and 0.7 mm. Fig. 5 shows the simulation results together with the experimental result.

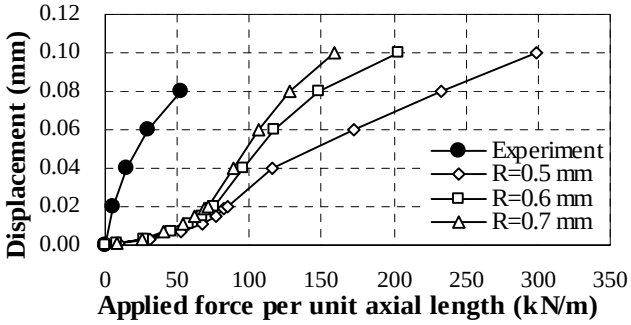

Fig. 5. The displacement of the upper plate as a function of the applied force per unit axial length. Simulations with the radius of the plates, R= 0.5, 0.6 and 0.7 mm were carried out.

All simulation curves can be considered to have two regions: below displacement of about 0.015 mm the simulation has a small slope; above 0.015 mm the results show a steep slope. The reason why these two regions exist can be explained by the two different tangent modulus of the generalized material property of the strand. Fig. 6 shows the stress-strain

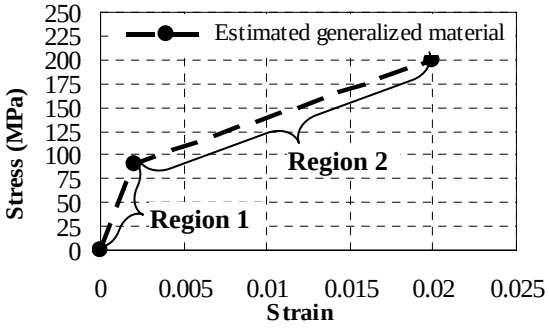

Fig. 6. The stress-strain curve of the estimated generalized material of the strand has region 1 and region 2.

curve of the generalized material property of the overall strand.

The tangent modulus of the region 1 results in the small slope of the simulation curves and the tangent modulus of the region 2 results in the deep slope of the simulation curves. Although the experimental curve shows no small slope region, its shape is very similar to that of the 0.6 and 0.7 mm curves above the displacement of 0.015 mm, as shown in Fig. 5. Therefore it is derived that the radius of the plates ranges from 0.6 to 0.7 mm in reality. The mismatch between the experimental curve and the simulation curves of 0.6 and 0.7 mm cases can be explained by the following reasons: the measurement of the displacement in the experiment has some uncertainties for very low displacements so it might not be possible to observe the small slope region; the material properties in the simulation have no ruptures; the voids or other structure defects in the strand reduce the stiffness of the strand and the thermal residual stress system in the strand after the heat treatment may affect the transverse stiffness of the strand. Fig. 7 shows the distribution of the total strain in the strand at the displacement of 0.1 mm. The strain value is overestimated, because the analysis does not take into account the ruptures of the materials. However, it still helps us locate the areas with high strains in the strand. The central sub-element has the highest strain and the areas with the strain value from 0.275 to 1.234 form an "X" shape in the strand. This is because under the compression the central sub-element yields first and the hexagonal shape of the sub-element decomposes the compression into a "X" shape.

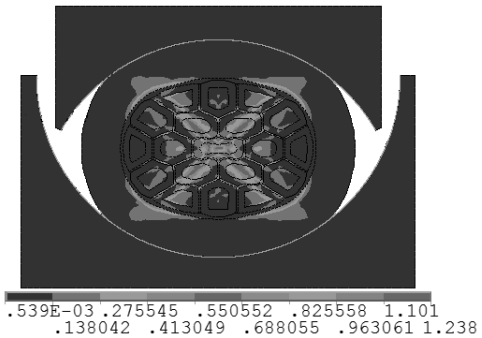

Fig. 7. The distribution of the total strain in the single strand at the compression displacement of 0.1 mm.

The two curves in Fig. 8 try to present a relationship between the high strain and the degradation of the normalized critical current measured in the experiment. The left y-axis is the normalized current, which is the ratio of the current of the strand under the compression to the case without load. The right y-axis is the number ratio of the nodes with total strain higher than an arbitrary value 0.15 in the superconducting filament areas to the all nodes in the filament areas in the FE model. As the displacement increases, the current performance almost has no degradation until 0.6 mm and starts to degrade at 0.6 mm. The number ratio maintains zero until 0.04 mm and then increase. Although the value 0.15 is arbitrary, the characteristic of the two curves indicates the degradation of the current is correlated with the high strain state in the strand.

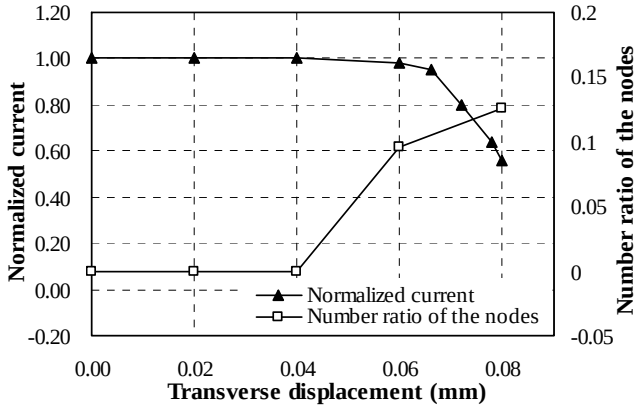

Fig. 8. Normalized current and number ratio of the nodes as a function of transverse displacement of the pressing plate.

B. Triplet simulation results

Fig. 9 shows the displacement vs. the applied force of the triplet simulation results compared to the experimental results. The results still show a mismatch, but the slopes are similar to each other, which means the tangent modulus of the region 2 of the generalized material in the FE model is close to the real modulus value of the cable.

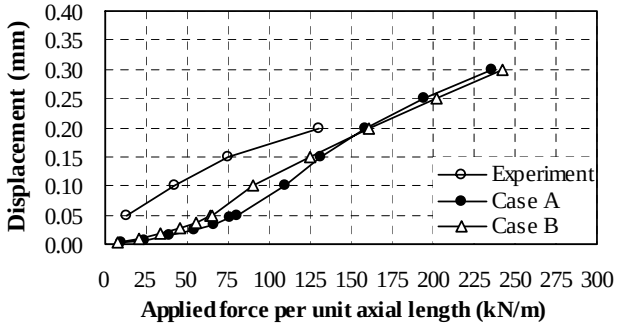

Fig. 9. Displacement as a function of applied force of triplet simulations and the experimental result.

The total strain distributions of case A and B are shown in Fig. 10 and Fig. 11. In case A, the high strain areas are distributed in every strand. In case B, strand 2 and strand 3 have more high strain areas than strand 1. In both cases, the sub-elements on the inside of each strand have higher strain than the outside sub-elements.

In order to understand which strand will have the largest current degradation (the numbering of the strand is shown in Fig. 3), Fig. 12 presents the number ratio of the nodes with total

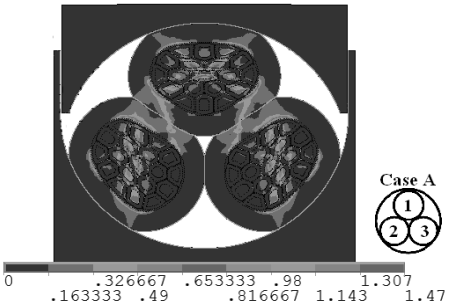

Fig. 10. The distribution of total strain in the superconducting filament areas of the case A at the compression displacement of 0.3 mm.

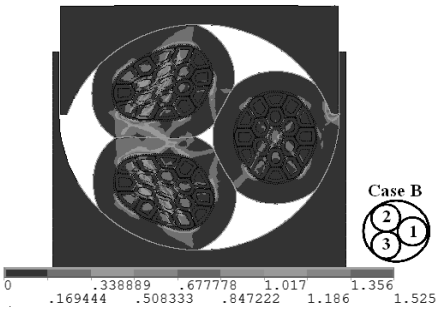

Fig. 11. The distribution of the total strain in the superconducting filament areas of the case B at the compression displacement of 0.3 mm.

strain higher than 0.1 in the filament areas to all the nodes in the filament areas of one strand in the triplet FE model. In case A, strand 1 has a higher ratio than that in strand 2 and strand 3. Therefore, strand 1 might cause the degradation of current performance firstly. This is reasonable because all applied force is reacted by the strand 1 in case A. In case B, strand 2 and strand 3 have a higher ratio than strand 1. This is also reasonable since almost all applied force is reacted by strand 2 and strand 3. It is concluded that strand 1 in case A and strand 2 and 3 in case B are the strands that have most potential to cause the current degradation for the triplet.

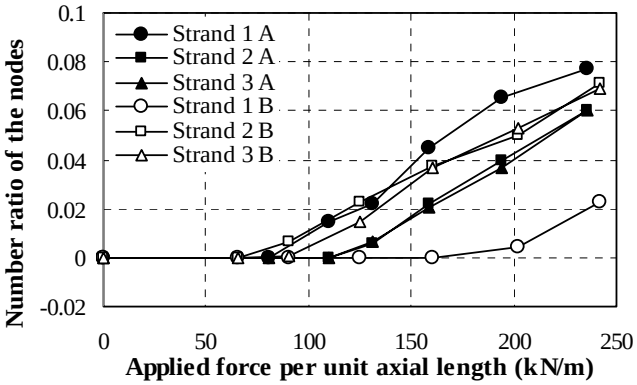

Fig. 12. The number ratio of the nodes with total strain higher than 0.1 to the total nodes in the superconducting filament areas of each strand in the triplet under transverse applied force.

Fig. 13 compares the node ratio of case A and case B. Y-axis presents the number ratio of the nodes with total strain higher than 0.1 to the all nodes in the superconducting filament areas

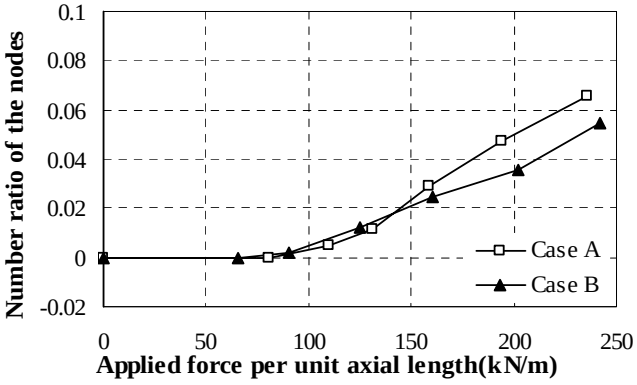

Fig. 13. The number ratio of the nodes with total strain higher than 0.1 to all the nodes in the superconducting filament areas of the triplet simulation.

in the triplet cable. Case A and case B have similar trends up to an applied force of 150 kN/m, while above it case A is assumed to have higher strain than case B.

V. CONCLUSION

FFA of Nb_3Sn single strand and triplet under transverse load is carried out to investigate the strain distribution in the strand(s). Although the strain value is overestimated as no material ruptures are taken into account in the analysis, the high strain areas in the strand(s) are obtained. In single strand the high strain areas form an "X" shape and the central sub-element has the highest strain. Based on the analysis of the number ratio of the nodes with high total-strain value higher than 0.1 to the all nodes in the filament areas under the transverse load, it is derived that the performance of the strand is correlated with the strain state in the strand. In the triplet cable, the cross section of the cable in longitudinal direction affect the strain state in a same strand. In case A, strand 1 has the highest strain but in case B, it has the lowest strain. However, under a same applied force, the effects of cases A and case B configurations on the strain state in the cable show a very similar behavior. This information can help in identifying which strand(s) degrades most and support current modeling efforts in this field. The results of the displacement vs. the applied force provide a way to compare the simulations and the experimental results. The trends of experimental and simulated curves are similar, which indicates the plastic modulus of the materials in FE model was appropriately chosen and it is close to the real value of the cable. We believe that the 2D results are promising but do not resemble all the characteristics of a real triplet because the simulation disregard the twisting effects. Future work will include 3-D simulations of the triplet to capture the effects of the twist on the strands.

VI. REFERENCES

[1] L. Chiesa, "Mechanical And Electromagnetic Transverse Load Effects On Superconducting Niobium-Tin Performance", Ph.D. thesis, Massachusetts Institute of Technology, 2009.
[2] http://www.roymech.co.uk/Useful_Tables/Tribology/co_of_frict.htm
[3] N. Mitchell, "Finite element simulations of elasto-plastic processes in Nb_3Sn strands", Cryogenics, vol. 45, No. 7, pp. 501–515, 2005.
[4] M. Poinier et al., "Elastic constants of polycrystalline Nb_3Sn between 4.2 and 300 K", Journal of Applied Physics, vol, 55 No. 9, pp. 3327-3332.
[5] D.S. Easton et al., "A prediction of the stress state in Nb_3Sn superconducting composites", Journal of Applied Physics, vol. 51, No.5, pp. 2748-2757.
[6] A. Nijhuis et al., "Systematic Study on Filament Fracture Distribution in ITER Nb_3Sn Strands", IEEE Tran. On Applied Superconductivity, vol.19, No.3, June 2009.